Very low frequency oscillations of heat load and recycling flux in steady-state tokamak discharge in TRIAM-1M

Hideki Zushi, Mizuki Sakamoto, Kazuaki Hanada, Yasuo Matsuo, Tatsuru Kuramoto, Tomoya Sugata, Nobuyuki Maezono, Hoshika Hirosi, Atsusi Iyomasa, Keisuke Sasaki, et al.

Very low frequency oscillations of heat load and recycling flux in steady-state tokamak discharge in TRIAM-1M

H. Zushi[a] , M. Sakamoto[a], K. Hanada[a] ,Y. Matsuo[b], K. Kuramoto[b], T. Sugata[b], N. Maezono[b], H. Hoshika[b], A. Iyomasa[a], K. Sasaki[b], K. Nakamura[a], K.N.Sato[a], H. Idei[a], S. Kawasaki[a], H. Nakashima[a], A. Higashijima[a] and M. Hasegawa[a]

[a]*Research Institute for Applied Mechanics, Kyushu University*

[b]*Interdisciplinary Graduate School of Engineering Sciences, Kyushu University*

Plasma wall interaction (PWI) driven relaxation oscillations are investigated in the steady state discharge for 5 hours. The oscillation frequency was about 10^{-3} Hz and each perturbation lasted for ~ 300 s. The heat load, recycling flux and impurity influx were varied from a few % to several tens of % . The largest variation of 70% was seen on the Mo XIII, although the influx of Mo I was only 20 %. Although the input rf power is kept constant during the discharge, the coupling between the rf and plasma was increased by ~ 10%. The current drive efficiency is decreased by 24 % in spite of current ramp. The toroidal and poloidal profiles of the recycling flux were also changed. During the last relaxation phase, the plasma was finally terminated. The current reduction (> 4 kA) was not recovered by intense local perturbation of the recycling superposed on the relaxation oscillation.

1. Steady State Tokamak Operation

With the goal of addressing the critical issues of steady-state tokamak operation (SSTO) [1] of future fusion devices, experiments aiming at 'day long operation at high performance' have been carried out in a limiter configuration of TRIAM-1M plasma (R_0 =0.84 m, a~0.12 m and B = 6-7 T). The plasma was maintained by lower hybrid wave LHW whose power of ~ 10 kW and the density was $1x10^{18}$ m^{-3}.The record value of the discharge duration was updated to 5 h and 16 min (Fig. 1). In order to investigate the main PWI and its effect on SSTO from a view point of heat load, particle recycling and impurity influx distributions, a rail limiter (movable limiter; ML) was inserted vertically into the plasma and thus the main contribution of the PWI could be localized on this. Other plasma facing components PFCs consist of three D-shaped limiters PLs, divertor plates DPs, vacuum vessel, the cover of bellows, and LH antenna. The ML and the one of PLs are located at the same port. The ML, PLs and DPs are made from molybdenum, and others are stainless-steel. The closest distances from the LCFS determined by the ML are ~5mm for the inner mid-plane part of PL, ~24 mm for outer one, ~46mm for DPs, 22mm for inner wall, ~41 mm for outer one, and ~46 mm for LH antenna, respectively.

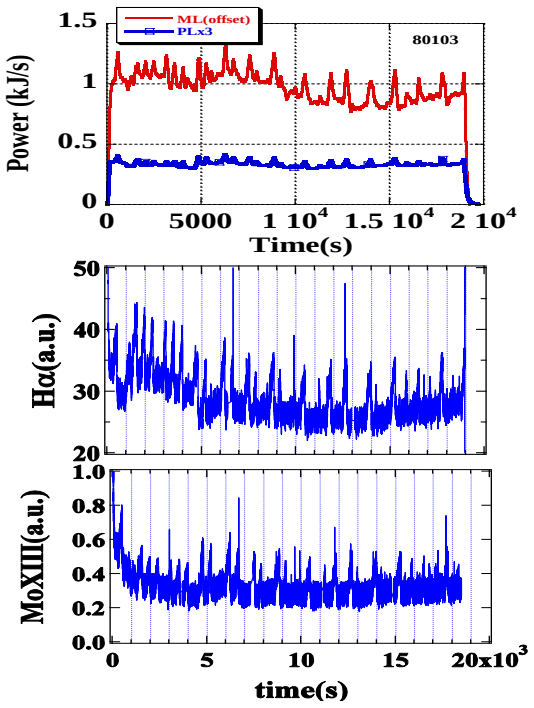

Fig. 1 Heat load, recycling flux and Mo XIII in five-hour discharge. Perturbations with 1-2x10^{-3} Hz are seen on these signals.

Heat and particle recycling fraction were determined by calorimetric measurement and H_α arrays around the torus[2,3]. A fraction of 34 % of the total heat load was deposited on the ML and the rest was distributed on PLs (10%), and wall (34%) and DPs (22%). The fraction of the recycling particle rate is ~40% from ML, 30% from PLs, and 30% from the wall and DPs. Thus the main heat load and particle flux are deposited mainly on the small area (a few cm^2) of the ML (3 cm in width and 16 cm in length along the major radius). The main metal impurity ions are Mo. Visible (Mo I 386 nm) and VUV (Mo XIII 34.1nm) spectrometers and soft X-ray array are used to investigate the impurity influx and accumulation in the core region. The influx of Mo I is determined ~ $3x10^{16}$ Mo atoms/ m^2 s. The surface and dust temperatures are measured by IR camera at 3.5 μm and a near IR spectrometer from

0.9 μm to 1.65 μm. By assuming bulk and dust temperatures (T_b and T_d) and surface coverage factor of dust for the viewing area, the observed near IR spectrum shows that T_d can reach the melting temperature of Mo and dusts cover a few % of the viewing area. During the discharge, the frequency of Mo spikes measured by influx monitor and soft X-rays increases toward the end. This shows that PWI during the discharge is not constant in time [3].

2. Ultra Low Frequency events

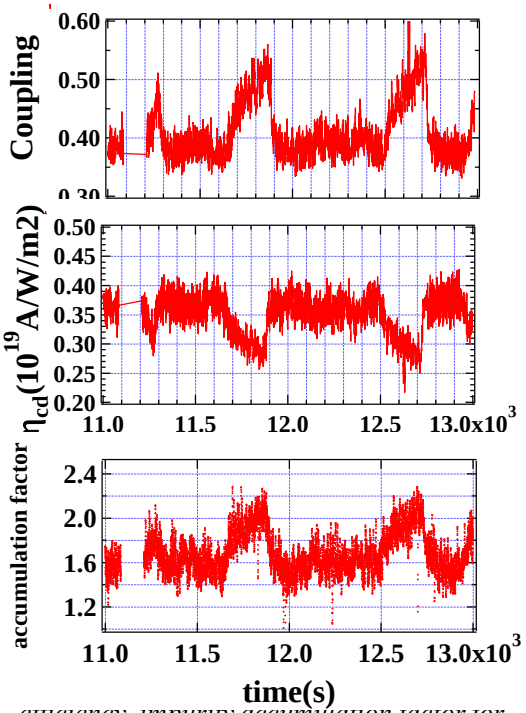

efficiency, impurity accumulation factor for ULF events.

As shown in Fig. 1, PWI driven relaxation oscillations (ULF events) are observed on heat load, recycling flux and impurity behaviour. These oscillations are semi-regular and should be distinguished from the random off-normal events, for example above mentioned impurity bursts. We are concerned with this oscillation because the 5 hour discharge has terminated during the last event (§3). ULF events are characterized by slow variations and quick decay. "Slow phase" lasts for 150 s ~ 200 s and "quick decay phase" ~ 100 s. ULF events are repeated at the frequency of 1-2x10^{-3} Hz. The unignorable power loss through the antenna made of stainless steel is taken into account to evaluate the net coupled power and it is observed that the coupling between the incident LHW power and the plasma maintains ~ 40 % whole duration, but increases to 50 % during the ULF event. As a consequence Ip and hard X-ray intensity integrated above 30 keV increase by ~ 3%. Thus, the current drive efficiency ($\eta_{CD}= I_p Rn_e / P$) with an assumption of the constant density shows a reduction from 0.37 to 0.28 x 10^{19} A/Wm^2. This unfavourable aspect is considered to be due to the impurity accumulation phenomenon. Here the accumulation factor, shown in Fig. 2, is defined as a ratio of MoXIII to Mo I, and as a consequence of the relatively large increment of Mo XIII it denotes that the injected impurity neutrals are accumulated during ULF events and lead to reduction in η_{CD} by enhanced collisions. The core impurity transport change during the ULF event, which is considered to be triggered by enhanced PWI, is under study.

A calorimeter system with 32 thermistors for cooling water temperature of PFCs were used to evaluate the distribution of the heat load deposited on the PFCs. The heat load on the ML starts to increase linearly at the rate of ~ 1.5±0.2 W/s when the ULF event occurs, and then decays at the same or lower rate. This aspect is different from those of the impurity or recycling flux. When we assume the interaction area of ~ 3 cm^2 for ML from CCD view the heat flux increases from 2.8 MW/m^2 to 3.3 MW/m^2 at the event. The heat load on other PFCs changes in similar manner at various changing rate. From the heat load measurement the heat fluxes <q> averaged on their interactive surface area are evaluated on each PFCs. The total heat load on the wall is the summation of the six part of the wall. The horizontal bar indicates each covering area. There seems an n=2-like toroidal structure.

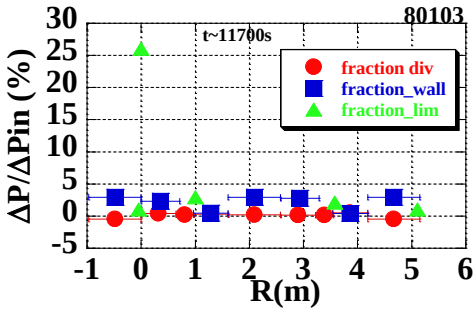

Fig. 3 The fraction distribution of the variation in heat load deposited on PFCs during the ULF event.

Although the covering areas of the two parts (Z~1.2m and Z~3.8m) of the wall are smaller than others, the <Δq(Z)> distribution also shows the similar structure. This structure remained for ULF events. The total power change ΔP_{in} in event is evaluated of ~ 1 kW from the net power evaluation, since the lost power in the antenna is decreased during ULF events. The summing up the total power change in all PFCs gives 0.44 kW, half the ΔP_{in}. The fraction of the heat load deposited on PFCs during the ULF events is shown in Fig.3. Although the missing power exists, the largest fraction was still localized on the ML.

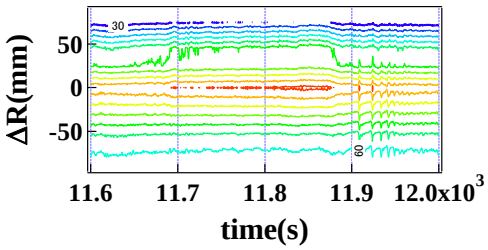

Fig. 4 The contour plot of $H_\alpha(\Delta R)$ during the ULF event.

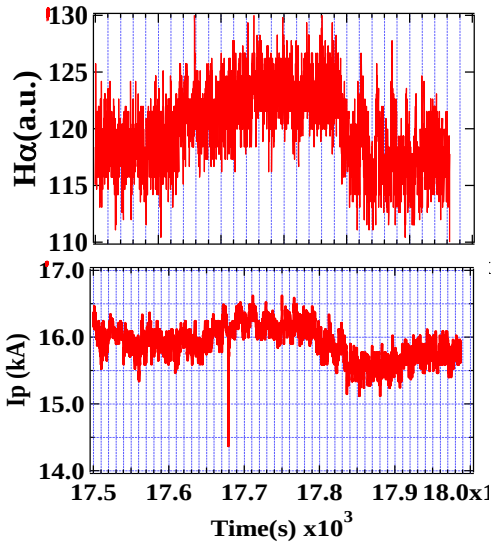

Fig.5 The one cycle of ULF event. Slow rise, quick decay, recovery phases are shown for H_α and Ip.

An H_α measurement system consists of fiber optics, narrow H_α filters and photomultipliers is used to measure toroidal (six positions) and poloidal (seven vertical chords) distributions. The ULF events are analyzed for the toroidal $H_\alpha(Z)$ (Z= a circumference of the torus) profile at $\Delta R=0$ and horizontal $H_\alpha(\Delta R)$ profile at Z=3.5m. As shown in fig.4, during the ULF event H_α increases in the longer R side and decreases in the shorter side, that is, $H_\alpha(\Delta R)$ shifts outward, which is favorable for rf coupling. The variation of H_α is 8% at $\Delta R=0$ and 35 % at $\Delta R=70$ mm. After a lapse of ~ 200 s from the trigger time of ULF event $H_\alpha(\Delta R)$ shifts back to the previous one within ~ 50 sec, but after that several bursts are seen. Their amplitudes are larger than the slow variation and decay in time for ~ 50 s. The each burst increases with a time constant of ~ 0.2 s and then decays with 0.7 s. The $H_\alpha(\Delta R)$ shifts inward at the burst, in the opposite direction compared to the slow variation. The $H_\alpha(Z)$ shows a highly localized profile near the ML, but the variation seems to be uniform around the torus, as shown in Fig. 7(a). In summary it is noted that the ULF event consists of three phases, slow increase and rapid decay following the relaxation phase. Namely, during the rapid decay phase the H_α and Ip are below the averaged ones, and therefore after that they recover gradually during the H_α bursts phase. This cycle is shown in Fig. 5. These cycles are repeated as ULF events.

3. Termination of the steady state discharge

The 5 hour discharge was stopped at $t=t_{end}$ (=19873.8 s) without a sign of termination. The last ULF event starts ~ -150 s before t_{end} and seems to continue similar to the previous ones. The heat load on the PFCs increase and the H_α also increases. Both $H_\alpha(Z)$ and $H_\alpha(\Delta R)$ profiles behave similary. These behaviors are within the variations of the previously repeated ones. An intense perturbation occurs t_1=-2.1s before t_{end}, as shown in Fig. 6. The current dropped by -25 % within 0.2 s, but it could be recovered to the previous level of 16 kA within continuing 0.8s. However, the second intense perturbation may trigger the current quench at t_2=- 1.1s. The current decayed gradually to ~10 kA for 1 s at the averaged quench rate of $dI/dt = -6kA/s$ and suddenly disrupted within 0.1 s. There is a different point in the current decay, namely for the first 0.2 s at both perturbations, the former decay rate is -20kA/s and the latter one is only 1kA/s. At the first perturbation the intense changes in the recycling fluxes are observed at the same time, but they delay by 0.2 s or 0.3 s with respect to the time at the current decays. Although the main recycling flux is supplied from the ML, the changes in the recycling flux are observed simultaneously around the torus. Figure 7 shows the $\Delta H_\alpha(Z)$ and $\Delta H_\alpha(\Delta R)$ profiles, the changed quantities from the averaged H_α levels before the ULF event is trigged. For reference the profiles at the ULF event (t=-3.8 s~-2.8 s) are shown. Outward shift

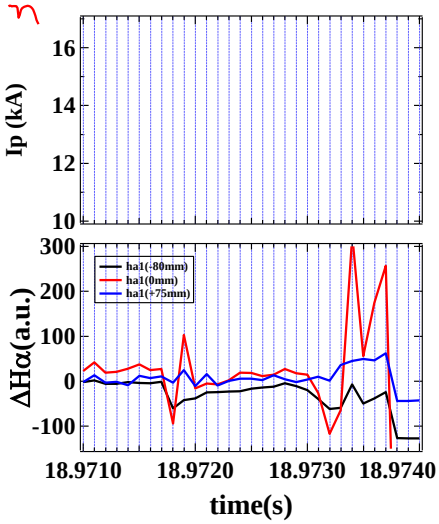

Fig.6 The two intense events ~ 2 s before the termination. The Ip drop, and relative variation of H_α at the ML are shown.

of $\Delta H_\alpha{}^9(\Delta R)$ and $\Delta H_\alpha{}^1(\Delta R)$ (not shown) and the almost uniform increment in H_α are similar to the above mentioned ones. At the first perturbation, $\Delta H_\alpha{}^9(\Delta R)$ shows a strong in-out asymmetry but $\Delta H_\alpha{}^1(\Delta R)$ does not show such one, indicating that the enhanced PWI in the outboard side occurs locally at the particular PFCs. The toroidal structure is quite complicated. At the ML the $\Delta H_\alpha(Z)$ is negative at t_1 and then becomes positive. $\Delta H_\alpha(Z)$ at the PL is always positive. The negative variation indicates the reduction in PWI. At the second perturbation above mentioned aspects in both profiles of $\Delta H_\alpha{}^9(\Delta R)$ and $\Delta H_\alpha(Z)$ are the same as the first one, but the amplitudes grows much resulting in final current quench.

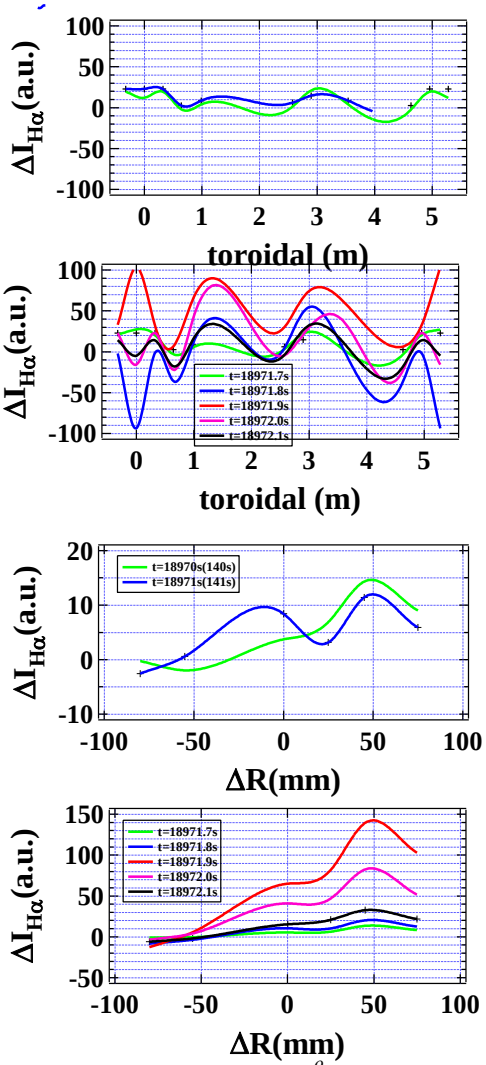

Fig.7 $\Delta H_\alpha(Z)$ (b) and $\Delta H_\alpha{}^9(\Delta R)$ (d) at the termination phase. For reference, profiles during the slow variation phase are shown (a) and (c).

Summary

The PWI driven relaxation oscillations and the termination of the discharge were investigated from a view point of SSTO. The 30~40 % of heat load and recycling particle flux are localized on the quite small area of the PFCs. The perturbations on heat load and particle recycling are repeated at the frequency of 1-2 $x10^{-3}$ Hz and the each event lasts for ~ 300 s. During the slow rise phase in the last event, intense two perturbations occurred at the particular location and the plasma could not be survived.

Acknowledgement

This work is partly supported by Grant-in-Aid for Scientific Research of Ministry of Education, Science, Sports and Culture Japan.

References

[1] H. Zushi et al., Nucl. Fusion **43** (2003) 1600.
[2] T. Kuramoto et al.,30th EPS **27A** (2003) P2 125.
[3] H. Zushi, T. Kuramoto et al., 31st EPS (2004).